Developmental Biology 393 (2014) 160–170

Contents lists available at ScienceDirect

Developmental Biology

journal homepage: www.elsevier.com/locate/developmentalbiology

CYCP2;1 integrates genetic and nutritional information to promote meristem cell division in *Arabidopsis*

Linda Peng [a], Anna Skylar [a], Peter L. Chang [a], Katerina Bisova [b], Xuelin Wu [a,*]

[a] Molecular and Computational Biology, University of Southern California, Los Angeles, CA 90089, USA
[b] Laboratory of Cell Cycles of Algae, Centre Algatech, Institute of Microbiology, Academy of Sciences of the Czech Republic, Třeboň, Czech Republic

ARTICLE INFO

Article history:
Received 12 March 2014
Received in revised form
31 May 2014
Accepted 11 June 2014
Available online 19 June 2014

Keywords:
Arabidopsis
CYCP2;1
STIP
Meristem
Cell division
Sugar signal

ABSTRACT

In higher plants, cell cycle activation in the meristems at germination is essential for the initiation of post-embryonic development. We previously identified the signaling pathways of homeobox transcription factor STIMPY and metabolic sugars as two interacting branches of the regulatory network that is responsible for activating meristematic tissue proliferation in *Arabidopsis*. In this study, we found that *CYCP2;1* is both a direct target of STIMPY transcriptional activation and an early responder to sugar signals. Genetic and molecular studies show that CYCP2;1 physically interacts with three of the five mitotic CDKs in *Arabidopsis*, and is required for the G2 to M transition during meristem activation. Taken together, our results suggest that *CYCP2;1* acts as a permissive control of cell cycle progression during seedling establishment by directly linking genetic control and nutritional cues with the activity of the core cell cycle machinery.

Introduction

The development of higher plants consists of two distinct phases. In the first phase, embryonic development sets up the basic body axes and sets aside one group of pluripotent cells near each end of the embryonic axis in the primary shoot and root apical meristems (Steeves and Sussex, 1989). Much knowledge has been gained in the past two decades regarding the molecular mechanisms involved in the specification of the primary meristems (reviewed in Rieu and Laux, 2009; Veit, 2004). Post-embryonic development, which is the second phase, is responsible for generating nearly all the organs found in an adult plant from the meristems. A key feature of a meristem is its ability to maintain cell division throughout a plant's life cycle, giving rise to new primordia and replenishing the stem cell population within.

For many plant species, the embryonic and post-embryonic stages are separated by seed desiccation, which renders the meristems silent in all cellular functions. Therefore, the primary meristems must activate cell cycle activities *de novo* immediately following germination, in order to reach their functional size and to initiate new organs (Medford, 1992). It has been demonstrated that, in *Arabidopsis thaliana*, the cells within the meristems arrest cell cycle in G1 prior to germination, and the core cell cycle machinery is reactivated starting with DNA replication at the time of germination (Barroco et al., 2005). Like other eukaryotic organisms, cell cycle decisions in higher plants rely on cyclin-dependent kinases (CDKs) and their interacting cyclins (CYCs). Five mitotic CDKs, CDKA;1, CDKB1;1, CDKB1;2, CDKB2;1, and CDKB2;2, are found in *Arabidopsis*, and all five have been shown to be involved in the establishment of a functional shoot meristem in the developing seedlings (Andersen et al., 2008; Barroco et al., 2005; Hemerly et al., 1995; Nowack et al., 2012). Expression and functional analyses suggest that the CDKs regulate different stages of the cell cycle, with CDKA;1 acting during both the G1 to S and G2 to M transitions, CDKB1 during G2, and CDKB2 at the G2 to M transition (Reviewed in Hemerly et al., 1995; Inagaki and Umeda, 2011; Menges et al., 2005; Porceddu et al., 2001). Similarly, different families of mitotic CYCs interact with the CDKs at specific points of the cell cycle to regulate CDK activities (Reviewed in De Veylder et al., 2007; Inzé and De Veylder, 2006).

The activities of the mitotic CYC-CDK complexes are influenced by a varietiy of signals, including the organism's nutritional state. In budding yeast, complexes between the minor CDK Pho85 and its interacting cyclins (Pcls) regulate cellular growth based on nutrient availability through a series of phosphorylation events (Carroll and O'Shea, 2002; Measday et al., 1997). Similarly, it has been demonstrated that stem cell division is regulated by both genetic and metabolic cues in animals as well as plants (Drummond-Barbosa and Spradling, 2001; Shim et al., 2002; Skylar et al., 2011). In higher plants, many pathways regulate

* Correspondence to: Molecular and Computational Biology, University of Southern California, Los Angeles, CA 90089-2910, USA. Fax: +1 213 740 8631.
E-mail address: xuelinwu@usc.edu (X. Wu).

http://dx.doi.org/10.1016/j.ydbio.2014.06.008
0012-1606/

meristem cell division by modulating the activities of the mitotic CDK and CYC (Reviewed in Inagaki and Umeda, 2011; Komaki and Sugimoto, 2012). Among them, metabolic sugars have long been known to promote meristem growth (Hanson and Smeekens, 2009; Lorenz et al., 2003; Moore et al., 2003; Paul et al., 2008; Van't Hof, 1966). At the cell cycle level, sugar activates the expression of key CYCs and CDKs that are required for both G1/S and G2/M transitions (Gaudin et al., 2000; Riou-Khamlichi et al., 2000; Skylar et al., 2011).

Previously, we identified the *Arabidopsis* homeobox transcription factor STIMPY (STIP/WOX9, referred to as STIP below, Haecker et al., 2004; Wu et al., 2005) as an essential gene in activating meristem growth at germination (Skylar et al., 2010; Wu et al., 2005). Seedlings that lack *STIP* fail to initiate cell division in the meristematic tissues due to a block at the G2 to M transition, a phenotype that can be rescued by the addition of metabolic sugars in the growth media (Wu et al., 2007, 2005). Expression profiling indicated that STIP and sugar signals share common downstream genes, suggesting that these two pathways merge before leading to cell cycle decisions (Skylar et al., 2011). Here we report the identification of the *CYCP2;1* (also called *CYCU1*, Torres Acosta et al., 2004; Wang et al., 2004), a Pcl homolog in *Arabidopsis*, as both a direct target of STIP transcriptional regulation and one of the early responders to sugar signal. We show that *CYCP2;1* promotes meristem cell cycle progression by directly interacting with the mitotic CDKs that are specific to the G2 to M transition.

Materials and methods

Plant materials

Plants were grown in long days (16 hours light/8 hours darkness) under about 120 $\mu E\ m^{-2}\ s^{-1}$ light at 22 °C. To observe seedling phenotypes, seeds were germinated on 1/2 Murashige Minimal Organics Medium (MS; Phytotechnology Lab) with 0.6% agar after two days of stratification at 4 °C. 44 mM of sucrose or sorbitol was used to assay for its effect on *CYCP2;1* expression. For callus cultures, excised root fragments were grown in ½ MS liquid media supplemented with 3% sucrose and 1 μg/ml 2,4-D, with slow agitation in the dark for two weeks at the room temperature. The *stip*-1 and *stip*-2 alleles were previously described (Wu et al., 2005).

Plasmid construction

*CL*13 was constructed by inserting the *GUS* coding sequence including the stop codon in-frame into the *BstBI* site 4 amino acids downstream of the *STIP* start codon, in the context of the 8.1 kb *STIP* genomic sequence (Wu et al., 2007). This fusion fragment was cloned into the binary vector *pJHA*212*K* (Yoo et al., 2005) and transformed into *Col*-0 plants. *ML*1*::STIP:GFP* was generated by fusing the 3.4 kb *ML*1 promoter (Sessions et al., 1999) with a *STIP:GFP* translational fusion (Wu et al., 2007) in *pJHA*212*K* and transformed into *stip*-2/+ plants. Transgenic lines that fully rescued homozygous *stip*-2 were selected for the callus cultures. *LP*01 and 35*S::Pcl*7 were constructed by inserting the full length cDNAs of *CYCP2;1* and *Pcl*7, respectively, into the binary vector *pCHF*3 (Fankhauser and Chory, 1997), then transformed into *Col*-0 and *LP*01-10 plants. *LP*39 was made by inserting the *CYCP2;1* coding sequence including the stop codon in-frame into the *BstBI* site 4 amino acids downstream of the *STIP* start codon in the context of the 8.1 kb *STIP* genomic sequence, and transformed into *stip*-2/+ plants. All transgenic lines were selected on MS medium containing 50 μg/ml kanamycin.

The C-terminal *GFP* fusion of *CYCP2;1*, *CDKA;1*, *CDKB2;1*, *CDKB2;2* were created by mutating each stop codon into a *NcoI* site, then fusing in-frame with the GFP cDNA at the C-terminus. The *GFP:CYCP2;1* fusion was made by fusing *CYCP2;1* to a modified *GFP* cDNA where the stop codon was replaced by a *NcoI* site. All split *YFP* fusions were generated by fusing the eYFP cDNA fragment encoding either amino acids 1-154 (YFP-N) or amino acids 155-238 (YFP-C) in-frame with the above cDNAs using the added *NcoI* site. All the fusions were expressed under the control of the constitutive *CaMV*35*S* promoter in *pCHF*3.

For yeast two-hybrid assays, *CYCP2;1* cDNA was fused to the *Gal*4 DNA-binding domain at the N-terminus in pDB-Leu (Invitrogen) at the *StuI* site. All five CDK cDNAs were fused to the *Gal*4 activation domain at the N-terminus in pEXP-AD-502 (Invitrogen) at the *SalI* site.

For insect cell expression, all five cDNAs were cloned into pENTR/SD/D-TOPO (Invitrogen) and recombined into BaculoDirect DNA using BaculoDirect™ C-Term Transfection Kit.

ChIP-seq and data analysis

The ChIP assay was performed according to Leibfried et al. (2005) with the following modifications. Calli were generated from the roots of *ML*1*::STIP:GFP* (experimental) and ML1:: NLS:2XGFP (control) in order to obtain sufficient amount of STIP-expressing tissue. The samples were fixed on ice under vacuum for 30 min with 1% formaldehyde before homogenization. The extracted chromatin was sheared to 100–600 bp fragments by sonication (Branson 250, output 3.5, duty cycle 20%). The GFP-bound DNA fragments were precipitated with anti-GFP antibodies (Abcam, ab290) and sequenced using an Illumina HiSeq system with 100-base single end reads after de-crosslinking.

Approximately 34 million and 37 million reads were obtained from the experimental and control samples, respectively. The reads were mapped to TAIR10 reference genome with RMAP (Smith et al., 2008), allowing at most 6 mismatches. The fraction of mappable reads was 58.7% and 67.7%, respectively. Mapping information was tabulated and the read depth at each genome position was calculated. The median depth in the control sample was 1.23X fold larger than the experimental sample. Thus, the experimental sample was scaled by a factor of 1.23X so that the ratio of both medians was 1. The genome was divided into non-overlapping 100 bp segments and the mean coverage depth for each segment was calculated. The mean coverage depth was then used to calculate the E/C coverage ratio to determine whether there is any enrichment of each segment in the experimental sample.

Histology and phenotypic analysis

GUS activity staining was carried out as described (Sessions et al., 1999), using 2 mM potassium ferro and ferri cyanide, at 37 °C for 12 to 14 h. For samples before seedling emergence, the embryos were removed from the seed coat for staining and mounted in 30% glycerol after staining for analysis.

Whole-mount *in situ* hybridization was performed as described (Friml et al., 2003) except that 10 ug/ml of proteinase K (Sigma-Aldrich # P2308) was used for digestion. *in situ* hybridization on tissue sections was performed as previously described (Lie et al., 2012). The Dig-labeled anti-sense probes used for *in situ* hybridization were generated by *in vitro* transcription using the full-length cDNA of each gene as the templates.

Samples were photographed on a Zeiss Axio Imager equipped with an AxioCam HRc camera and whole seedlings were imaged using a Leica M165FC stereomicroscope with a DFC295 camera.

Flow cytometry analysis was done as previously described (Wu et al., 2007).

Real-time RT-PCR

Total RNA was extracted using the Spectrum Total Plant RNA Kit (Sigma), and the first-strand cDNA was obtained using the Enhanced Avian First Strand Synthesis Kit (Sigma). Real-time PCR was carried out with the SYBR-green (Molecular Probes) method on Opticon-2 MJ machines. The relative changes in gene expression levels were determined using the $2^{-\Delta\Delta CT}$ method. Each sample was done in at least two biological replicates, each with three technical replicates, and either *ACTIN*8 (Puthiyaveetil and Allen, 2008) or *eIF4A* (*At*3*g*13920) was used for normalization. The primers used in this study are:

*CYCP*2;1: 5′-cgaaaactctaaaactcacagtaactctaa-3′ and 5′-ctagatgacgt*gcactacaacaac-3′
*ACT*8: 5′-ttccagcag*atgtggatctcta-3′ and 5′-agaaagaaatgtgatcccgtca-3′;
eIF4A: 5′-cagcaaagaggaatcgtcccct-3′ and 5′-gcctgacactggataagggagaagt-3′.

Asterisk (*) indicates exon-intron boundary.

Protein-protein interaction assays

Yeast two-hybrid analysis was carried out according to the PROQUEST two-hybrid system manual (Invitrogen). Transient expression in *N. benthamiana* leaf cells was done according to Voinnet et al. (2003) with the following modifications. *Agrobacterium* cells were resuspended in infiltration media containing 10 mM $MgCl_2$ and 10 mM MES to a final O.D. of 0.5 for the strains carrying the expression constructs and 0.3 for the strain carrying p19. The cell mixture was activated with 200 μM acetosyringone for 2–4 h at room temperature before infiltration. Fluorescence signals were imaged using a Leica SP8 confocal microscope.

Kinase assay

For kinase activity assays, insect Sf-9 cells were transfected with recombinant BaculoDirect DNA containing cDNAs C-terminally tagged with 6xHis and V5 epitope. The infected cells were collected in ice cold PBS 2 or 3 days postinfection, fast frozen in liquid nitrogen and stored at −20 °C until the assay. CDK-cyclin complexes were purified using Ni-NTA agarose (Qiagen) under native conditions according to manufacturer's instructions. Purified complexes immobilized on Ni-NTA agarose were washed twice with kinase buffer (20 mM HEPES (pH 7.5), 15 mM $MgCl_2$, 5 mM EGTA, 1 mM DTT); the kinase activity was measured according to Bisova et al. (2005). Phosphorylated histone bands were separated by SDS-PAGE and detected by phosphoimager (Molecular Dynamics). For each protein combination, results from six to eight independent pull-downs were averaged for comparison.

Results

STIP is an activator of CYCP2;1 expression at the time of germination

In order to understand how STIP regulates meristem cell cycle activation, we set out to identify the genomic loci occupied by STIP using chromatin immune-precipitation followed by deep sequencing (ChIP-seq). In wildtype *Arabidopsis*, *STIP* is transiently expressed in very limited tissues and the plants do not tolerate high levels of *STIP* over-expression. To overcome these limitation, we generated *stip*-2 mutants that also expressed a STIP:GFP fusion protein under the control of the *AtML*1 promoter, as our experimental sample. Because of the significant overlaps between the *STIP* and *ML*1 expression domains, the *ML*1::*STIP:GFP* transgene was able to fully rescue the seedling phenotype of the *stip*-2 mutants and resulted in a very mild *STIP* over-expression phenotype at the leaf margin (data not shown). A NLS:2xGFP expressed under the same promoter (Wu et al., 2003) was used as a control for non-specific binding. The experimental/control coverage ratio of a given chromosomal location, as calculated in a 100 bp sliding window, was used to identify regions with significant STIP-binding. One of these segments with approximately 5-fold enrichment in the experimental sample, which is within the upper 2% of the genome-wide distribution of fold change (Fig. S1), was found to be centered 400 bp upstream of the coding region of *CYCP*2;1 (*At*3*g*21870, Fig. 1A). In addition, it was flanked by two other segments with fold enrichment of 3.2 and 4.1 (upper 2.7% and 2%), suggesting that this region of the genome likely contains true binding sites of STIP and that *CYCP*2;1 may be a direct target of STIP regulation.

If STIP is a regulator of *CYCP*2;1 transcription, we expect to find them expressed in overlapping domains. Because the *stip* mutant phenotype becomes apparent immediately after cotyledon opening, we focused our attention on the time of seedling emergence, which is between 50–60 h after stratification under our growth conditions. *CL*13, a β-glucuronidase (GUS) reporter, in which *GUS* was transcriptionally fused to the *STIP* coding region in the context of the 8.1 kb *STIP* genomic sequence (Wu et al., 2007), was used to monitor *STIP* promoter activity. In newly emerged seedlings, high levels of STIP::GUS activities could be detected in the cotyledons, the top portion of the hypocotyl, and the upper region of the root meristematic zone (Fig. 1D). At the same stage, *in situ* hybridization detected *CYCP*2;1 mRNA in the cotyledons and the L1 layer of the shoot meristem (Fig. 1E), and also in the upper root meristematic and transition zones (Fig. 1C). In addition, a *CYCP*2;1 expression time course using real-time RT-PCR (qRT-PCR) showed that the *CYCP*2;1 mRNA level was 3–4 fold higher in the wild type than in *stip*-1 mutants before cotyledon greening, which is approximately 72 h post-stratification (Fig. 1B). Both the overlapping expression domains and the early reduction in *CYCP*2;1 transcription indicate that STIP is involved in activating *CYCP*2;1 expression at the time of germination.

However, after cotyledon greening, a significant increase in *CYCP*2;1 levels was observed in both the wildtype and the *stip* mutant seedlings (Fig. 1B). Additional analyses showed that this increase likely occurred in the above-ground tissue, where *CYCP*2;1 continued to be expressed in the cotyledons, the shoot apex, and the young leaves (Fig. 1F; data not shown). In comparison, *STIP* is undetectable in the above ground tissues at this stage except for a transient expression in the shoot meristem (Wu et al., 2005), suggesting that additional mechanisms activate *CYCP*2;1 transcription in the shoot after the completion of germination.

Ectopic CYCP2;1 expression partially rescues stip mutants

To determine how much the reduced *CYCP*2;1 expression in *stip* mutants is responsible for its seedling growth arrest phenotype, we expressed *CYCP*2;1 in *stip*-2 background in the endogenous *STIP* expression domain by transcriptionally fusing *CYCP*2;1 cDNA to the *STIP* coding region in the context of the 8.1 kb *STIP* genomic sequence (*LP*39). Due to the ovule defects caused by the loss of *STIP*, the transgenic lines were assayed for any possible rescue effect in *stip*-2/+ segregating populations based on the percentage of seedling growth arrest, in the T2 generation (Table 1). Among the offspring of *stip*-2/+ plants, nearly 30% arrest growth at germination, resulting in a healthy/arrested seedling ration of

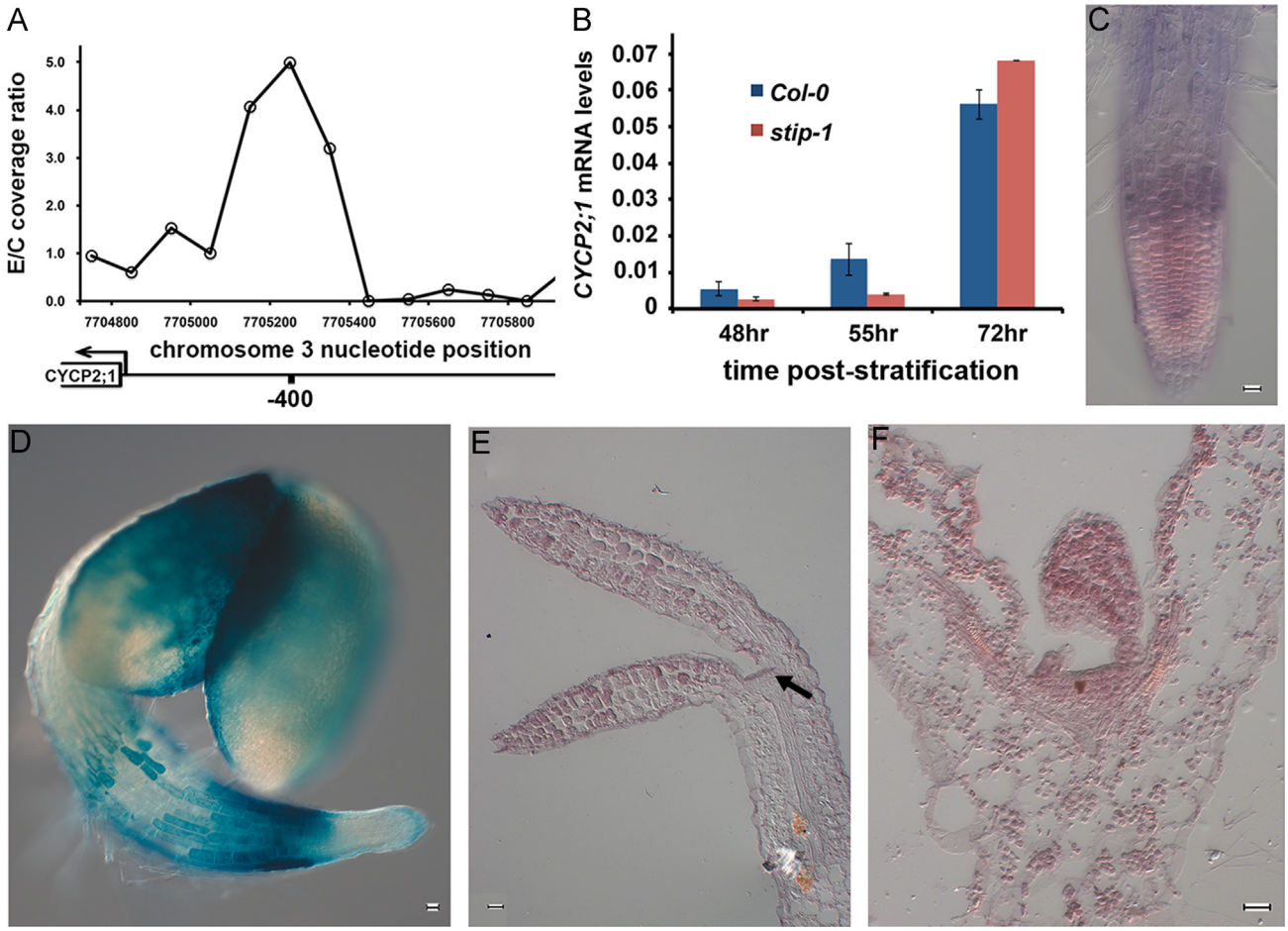

Fig. 1. STIP activates *CYCP2*;1 transcription at germination. (A) A peak of STIP-binding was detected approximately 400 bp upstream of *CYCP2*;1 coding region using ChIP-seq. (B) *CYCP2*;1 mRNA levels relative to the levels of *eIF4A* in germinating *Col*-0 and *stip*-1 seedlings, as detected by qRT-PCR. The three time points correspond to different stages during the germination process. 48 h marks the beginning of germination, when the radicle protrudes out of the seed coat. Around 55 h, the seedlings have fully emerged from the seed coat, with closed apical hooks and cotyledons. By 72 h, the cotyledons are fully open and green. (C) Whole-mount *in situ* hybridization of *CYCP2*;1 with an antisense probe in the root of 55 h post-stratification *Col*-0 seedlings. (D) *STIP::GUS* activities in 55 h post-stratification *Col*-0 seedlings. (E, and F) *in situ* hybridization of *CYCP2*;1 with an anti-sense probe in the shoot of 55 h post-stratification (E) and 2-day-old (F) *Col*-0 seedlings. Arrow in (E) points to *CYCP2*;1 expression in the shoot meristem. Scale bar represents 20 μm.

Table 1
CYCP2;1 expressed under the *STIP* promoter partially rescues *stip*-2 mutants.

Genotype	*stip*-2/+	*LP*39 in *stip*-2/+							*stip*-2	*LP*39 in *stip*-2	
line #		5	6	8	10	11	16	17		4	14
Healthy seedlings	659	165	293	241	96	201	194	168	17	132	151
Arrested seedlings	278	18	57	39	19	42	33	39	233	65	50
Healthy/arrested	2.4	9.2	5.1	6.2	5.1	4.8	5.9	4.3	0.073	2.0	3.0

Note: *P*-value <0.003 based on Fisher's exact test.

2.4. Of the 20 independent *stip*-2/+ T2 lines carrying *LP*39, 7 had a higher than 4 ratio between healthy and arrested seedlings, which indicated a significant improvement from *stip*-2/+ (*P* value <0.003). A more dramatic rescue effect was observed in two *LP*39 T2 lines that were homozygous for *stip*-2. When compared to the *stip*-2 offspring that survive past embryogenesis, among which only approximately 7% initiate post-embryonic development, the *LP*39 transgene was able to increase the seedling survival rate to 67% and 75%, respectively. Using qRT-PCR, we found that *CYCP2*;1 was expressed at approximately twice the wildtype levels in both lines at 56 h post-stratification (Fig. S2A). These results support the conclusion that the reduction of *CYCP2*;1 expression in *stip* mutants at the time of emergence is at least partially responsible for the seedling growth arrest phenotype in *stip* mutants, and that *CYCP2*;1 is one of the major effectors downstream of *STIP* during seedling growth activation.

Loss of CYCP2;1 results in seedling growth arrest upon emergence

Unfortunately, no knock-out allele of *CYCP2*;1 exists in the T-DNA insertion collections. Instead, we assessed its function using ectopic expression driven by the constitutive *CaMV35S* promoter. Two classes of phenotype were observed in 32 independent transgenic lines carrying *35S::CYCP2*;1 (*LP*01). 22 lines were indistinguishable from the wild type throughout their life cycle (Fig. 2B, compare to A). Based on qRT-PCR results, their *CYCP2*;1

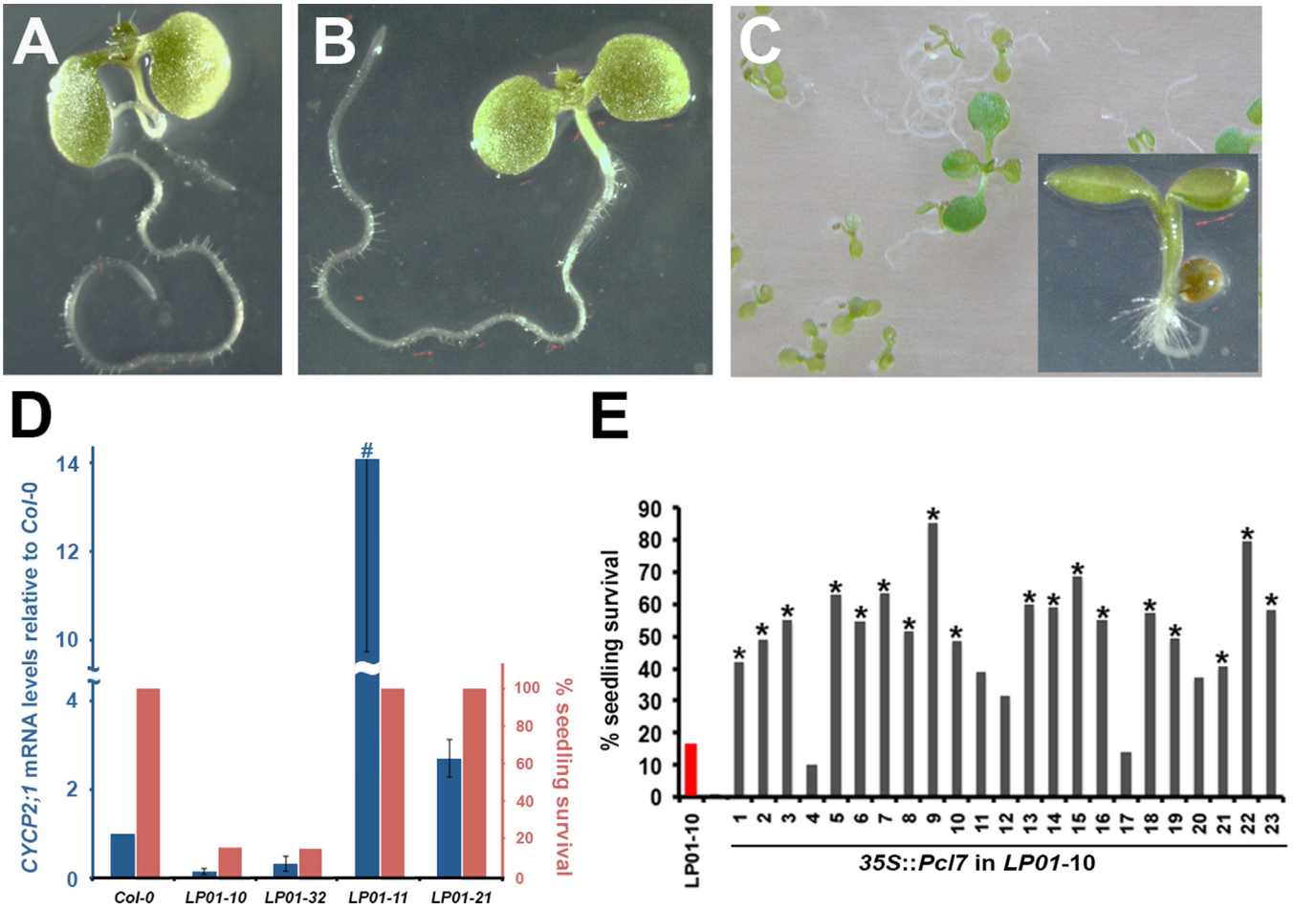

Fig. 2. Loss of *CYCP*2;1 results in seedling growth arrest following germination. (A and B) 5-day-old *Col*-0 (A) and *CYCP*2;1 over-expression (B) seedlings on MS media. (C) The majority of *LP*01-32 seedlings arrest growth at germination on MS media. Inset: a 5-day-old arrested seedling at the same magnification as in (A) and (B). (D) Blue: relative *CYCP*2;1 mRNA levels in 1-day-old seedlings of *Col*-0 and selected *LP*01 lines. The wildtype control was artificially set at 1. All samples were normalized to *ACT*8. #: only one tail of the error bar is shown for this line. Red: seedling survival rate of the corresponding genotypes. (E) Seedling survival rate of *LP*01-10 and the independent T2 lines over-expressing *Pcl*7. * indicates the lines in which *P* value < 0.001.

expression levels ranged between two to fifty folds of that of the wildtype samples at 72 h post-stratification (two example, *LP*01-11 and *LP*01-21, are shown in Fig. 2D). This led us to the conclusion that elevated *CYCP*2;1 levels do not affect plant development. In the remaining 10 lines, 10% to 90% of seedlings arrested growth following germination. Phenotypically, these growth-arrested seedlings appeared identical to the *stip* mutants, with no sign of development in either the shoot or the root (Fig. 2C, Wu et al., 2005). In the transgenic lines with large percentage of seedling arrest, the levels of *CYCP*2;1 transcript, including both the endogenous and from the transgene, were significantly reduced when compared to the wild type (two example, *LP*01-10 and *LP*01-32, are shown in Fig. 2D). The most likely cause for this observed reduction in expression is transgene-induced silencing. Because no gene in the *Arabidopsis* genome shows significant sequence homology to *CYCP*2;1 at the nucleic acid level, it is unlikely that any gene other than *CYCP*2;1 was silenced in these plants. Furthermore, when we compared the mRNA levels of all seven *P*-type cyclins in newly emerged *LP*01-10 and *stip*-1 to the wild type, only *CYCP*2;1 was found to be reduced in *LP*01-10 or *stip*-1, supporting the conclusion that the observed seedling arrest phenotype was due to the loss of *CYCP*2;1. Because the phenotype of these *CYCP*2;1 silencing lines are stably transmitted through generations, we treat them as loss-of-function *CYCP*2;1 alleles in this study.

The *P*-type cyclins share approximately 40% identity with the yeast Pcl proteins in their Cyclin_N domains (Torres Acosta et al., 2004). Based on amino acid sequences, the closest homolog of CYCP2;1 in *S. cerevisiae* is Pcl7, which links cell cycle decisions with carbohydrate availability (Lee et al., 2000). To determine the level of functional conservation between CYCP2;1 and Pcl7, we ectopically expressed *Pcl*7 under the *CaMV*35*S* promoter in *LP*01-10 plants to test whether it can compensate for the lack of *CYCP*2;1. Without ectopic *Pcl*7, more than 85% of *LP*01-10 plants ($N=421$) arrest growth at germination. In comparison, 18 of the 23 independent T2 lines expressing *Pcl*7 were able to reduce the growth arrest rate to below 60% (Fig. 2E), indicating significant rescue of the parental phenotype (*P* value < 0.001). This finding not only shows that the molecular functions of CYCP2;1 and Pcl7 are partially conserved across the kingdoms, but also supports our previous conclusion that the seedling growth arrest phenotype in *LP*01-10 and its sibling lines was caused by the loss of *CYCP*2;1.

CYCP2;1 is required for seedling meristem growth activation

The mutant phenotypic resemblance and the genetic relationship between *CYCP*2;1 and *STIP* suggest that *cycp*2;1 mutants suffer a general failure in seedling growth initiation, as was observed in *stip* mutants. To test this hypothesis, we compared cell cycle gene expression levels in the meristematic region of

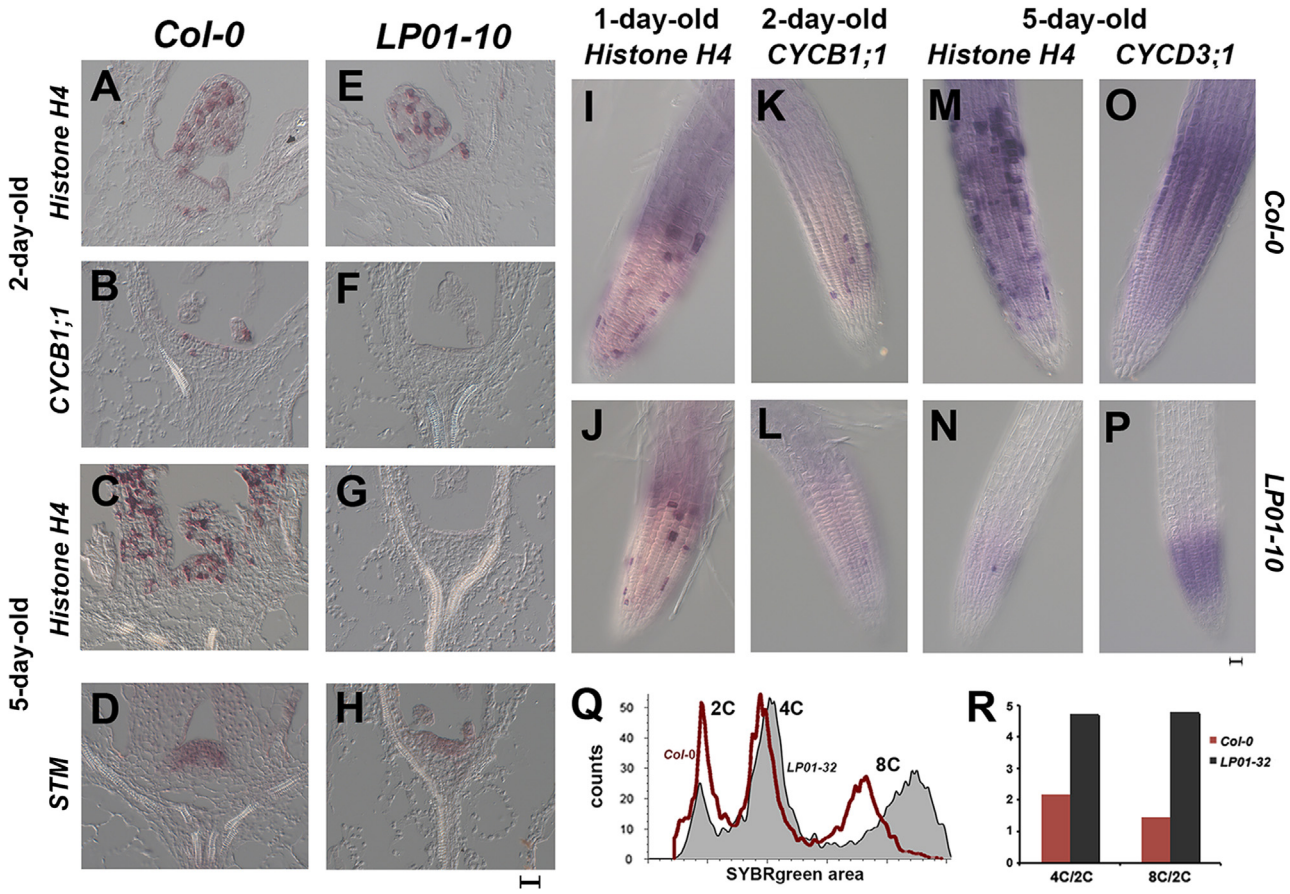

Fig. 3. Loss of *CYCP2*;1 leads to failure in seedling meristem growth activation. (A–H) *Histone H4*, *CYCB1;1*, and *STM* mRNA patterns detected using anti-sense probes in the shoot meristems of 2-day-old and 5-day-old *Col*-0 (A–D) and *LP*01-10 (E–H) seedlings. (I–P) *Histone H4*, *CYCB1;1*, and *CYCD3;1* mRNA patterns detected using anti-sense probes in the root meristems of 1-day-old and 5-day-old *Col*-0 (I,K,M, and O) and *LP*01-10 (J,L,N, and P) seedlings. (Q) Nuclear DNA content in 7-day-old *Col*-0 and *LP*01-32 roots, as measured by flow cytometry. The shift in the position of the 8C peaks between the two samples is likely due to differences in the shape of the nuclei. (R) Ratios between nuclei of different ploidy from wild-type and *LP*01-32 roots. The *LP*01-32 sample has a significantly higher ratio of tetraploid (4C) or octaploid (8C) nuclei to diploid (2C) nuclei. Scale bar represents 20 μm.

*LP*01-10 and wildtype seedlings at different times after germination. Two days after germination, similar levels of *Histone H4* expression, which marks DNA synthesis, was detected in the shoot meristems of the two genotypes (Fig. 3A, and E). At the same time, little to no *CYCB1;1* mRNA could be found in the *LP*01-10 shoot meristems (Fig. 3F, compare to B), indicating a lack of mitotic activation. Three days later, the wildtype shoot meristem has grown into the typical dome-shaped structure as marked by the expression of *SHOOT MERISTEMLESS* (*STM*; Fig. 3D), and *Histone H4* mRNA could be detected in all the growing tissue around the shoot apex (Fig. 3C). In contrast, the shoot meristems of 5-day-old *LP*01-10 seedlings remained in the same shape and size as the ones found in 2-day-old samples (Fig. 3G, and H). While the *Histone H4* expression is completely lacking in their shoot apices (Fig. 3G), *STM* is still activated in the mutants, suggesting that the cells in their shoot meristems remain undifferentiated, but arrested cell cycle instead. A similar scenario was observed in the root meristem as well. One day after germination, the *LP*01-10 root meristems have the morphology and *Histone H4* expression that were very similar to what was observed in the wildtype seedlings (Fig. 3I, and J). However, the majority of the *LP*01-10 roots showed no *CYCB1;1* expression two days after germination, when it became detectable in the wild type (Fig. 3K, and L). By five days post-germination, *Histone H4* is no longer detectable in *LP*01-10 roots (Fig. 3N, compare to M). However, *CYCD3;1* is still expressed in the much reduced root meristem region in these mutants (Fig. 3P, compare to O), suggesting that these cells still have G1 to S activity and are not differentiated. Since the expression profiles of these core cell cycle genes suggest that the cells in *LP*01-10 meristem likely arrested cell cycle in G2, we examined the nuclear DNA content of root nuclei that were isolated from wildtype and growth-arrested *LP*01-32 seedlings by flow cytometry. As shown in Fig. 3Q, nuclei size distribution clearly indicated a reduction in the number of 2C nuclei in *LP*01-32. Further analysis showed that the ratio between the number of 4C and 2C nuclei in *LP*01-32 have nearly doubled from the widltype level of 2.18 to 4.73 (Fig. 3R), confirming a G2 arrest in *cycp2;1* mutants.

CYCP2;1 physically interacts with selected mitotic CDKs

At the amino acid level, *CYCP2;1* encodes a cyclin-like protein with only the CYCLIN_N domain, which is responsible for carrying out physical interactions with the CDK proteins (Lees and Harlow, 1993). It has been reported that CYCP2;1 can interact with CDKA;1, but not with CDKB1;1, in yeast-two hybrid assays (Torres Acosta et al., 2004). The G2 cell cycle arrest in *cycp2;1* mutants led us to further test CYCP2;1 interaction with all five *Arabidopsis* mitotic CDKs in yeast by fusing CYCP2;1 to the GAL4 DNA-binding domain (DB) and the CDK proteins to the GAL4 activation domain (AD). As shown in Fig. 4A, only background level of His reporter activities were detected between CYCP2;1 and CDKB1;1, CDKB1;2. In comparison, significantly stronger activation of the His reporter

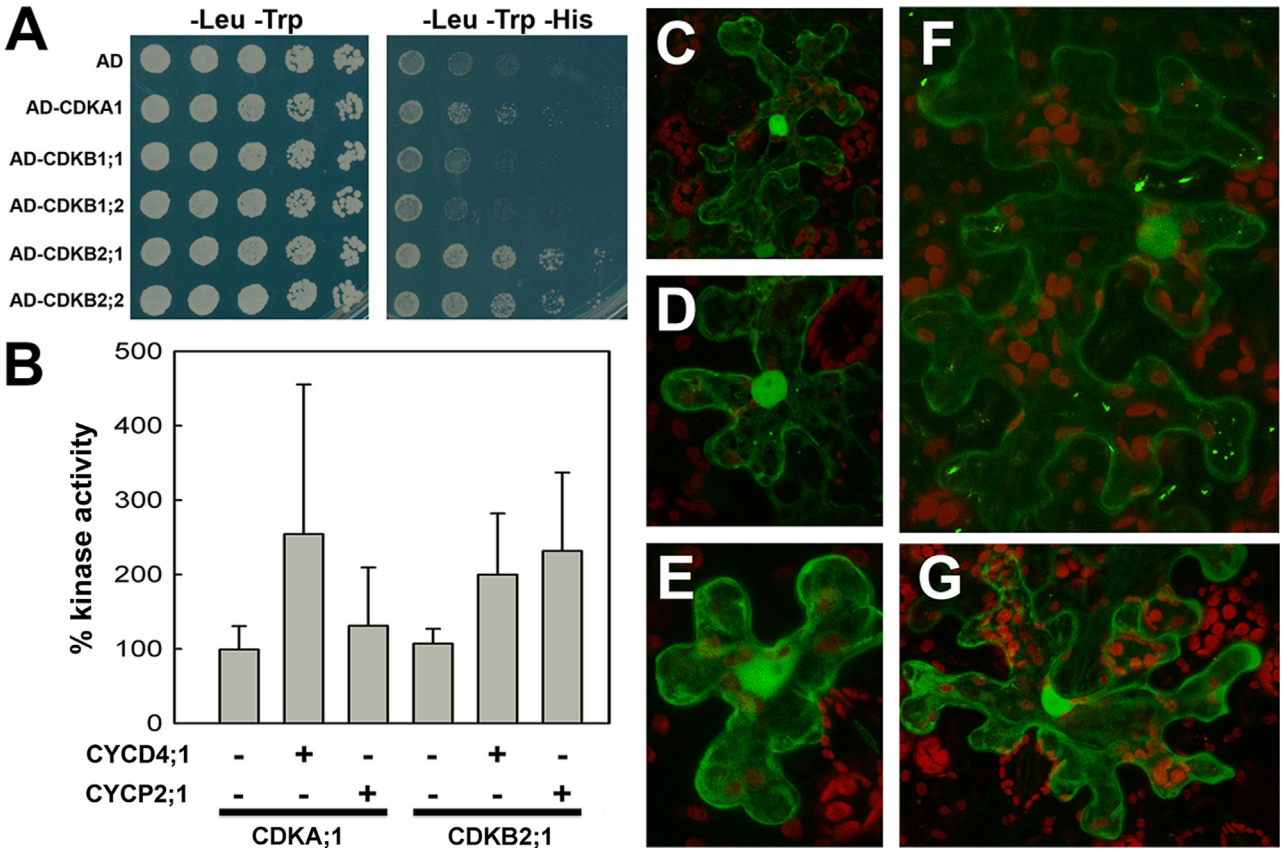

Fig. 4. *CYCP*2;1 physically interacts with three mitotic CDKs. (A) *CYCP*2;1 interacts with CDKA;1, CDKB2;1, and CDKB2;2 in yeast two-hybrid. The left panel shows 5-fold serial dilutions of the cells grown on media that selects for the presence of the bait and prey plasmids. The right panel shows the same cells on media that selects for cells in which the bait and prey interaction resulted in the activation of the His3 reporter. (B) Quantified kinase activities of *CYCP*2;1 and CYCD4;1 complexed with CDKA;1 and CDKB2;1 in insect cell cultures, using histone H1 as the substrate. Each group of samples was normalized to the CDK-only control, which was artificially set as 100%. (C–D) Maximum projections of confocal images of *CYCP*2;1:GFP (C) and CDKA;1:GFP (D) in tobacco leaf epidermal cells. The red channel detects chloroplast auto-fluorescence. (E–G) Maximum projections of confocal images of tobacco leaf epidermal cells transiently co-expressing *CYCP*2;1:YFP-N with CDKA;1:YFP-C (E), CDKB2;1:YFP-C (F), and CDKB2;2-YFP-C (G) in BiFC assays. The nuclear YFP signals indicate physical interaction between the two proteins. The red channel detects chloroplast auto-fluorescence.

was found between CYCP2;1 and CDKA;1, CDKB2;1, CDKB2;2, suggesting that CYCP2;1 physically interacts with these three CDKs.

We further confirmed the physical interaction between CYCP2;1 and the three CDKs *in planta* using the bimolecular fluorescence complementation (BiFC) assay (Hu et al., 2002) via *Agrobacterium*-mediated transient expression in tobacco leaf epidermal cells. Like the CDK:GFP fusions, CYCP2;1 was mainly localized to the nucleus when fused to GFP at either the N- or C- terminus (Fig. 4C, and D, data not shown, Boruc et al., 2010). To carry out the BiFC assay, CYCP2;1 was fused to the N-terminal portion of eYFP (YFP-N), and the CDKs were fused to the C-terminal portion of eYFP (YFP-C). Each CDK:YFP-C fusion was co-expressed with CYCP2;1:YFP-N, and free YFP-N and YFP-C were used as negative controls for background fluorescence detection. In leaves co-transfected with the CYCP2;1 and CDKA;1 fusions, approximately 50% of the cells within the infiltration sites showed strong nuclear YFP signal (Fig. 4E). In contrast, no YFP signal was detected in cells infiltrated with CYCP2;1:YFP-N and YFP-C, and fewer than 10% of cells at the sites infiltrated with CDKA;1:YFP-C and YFP-N developed weak nuclear YFP signal. Similar results were observed between CYCP2;1 and the two CDKB2s, where approximately 40% of the cells co-infiltrated with CYCP2;1:YFP-N and CBKB2;1:YFP-C or CDKB2;2:YFP-C showed clear nuclear YFP signal (Fig. 4F, and G) and little to no background fluorescence was detected. These observations support the conclusion that CYCP2;1 physically interacts with CDKs that act during the G2/M transition in plant cells.

CYCP2;1-binding activates CDKB2;1

In *S. cerevisiae*, Pcl-binding to Pho85 results in active complexes that are able to phosphorylate selected substrates (Kaffman et al., 1994; Lee et al., 2000; Measday et al., 1994). To test whether CYCP2;1 activates the kinase activities of its interacting CDKs, we affinity purified CDKA;1 and CDKB2;1 from Sf9 cell lysate that co-expressed CYCP2;1, and examined their ability to phosphorylate the generic substrate histone H1. As a positive control, the CDKs were also co-expressed with CYCD4;1, a mitotic cyclin that has been shown to interact with both of them (Boruc et al., 2010; Kono et al., 2003). As shown in Fig. 4B, background levels of kinase activities were detected when only a CDK was expressed in the culture, and the two CDKs responded differently to the binding of the two cyclins. Both CYCD4;1 complexes, CDKA;1-CYCD4;1 and CDKB2;1-CYCD4;1, were able to phosphorylate histone H1 at high levels ($P < 0.1$ and $P < 0.05$, respectively), confirming the previous results (Kono et al., 2003). Similarly, the CYCP2;1-CDKB2;1 complex had significantly higher kinase activities than the CDK-only control ($P < 0.05$). However, the activity of CDKA;1-CYCP2;1 complex was not significantly higher than the control. This suggests that the CYCP2;1/CYCD4;1-CDKB2;1 complexes act in a similar mechanism using similar substrates, and CDKA;1 activity is highly

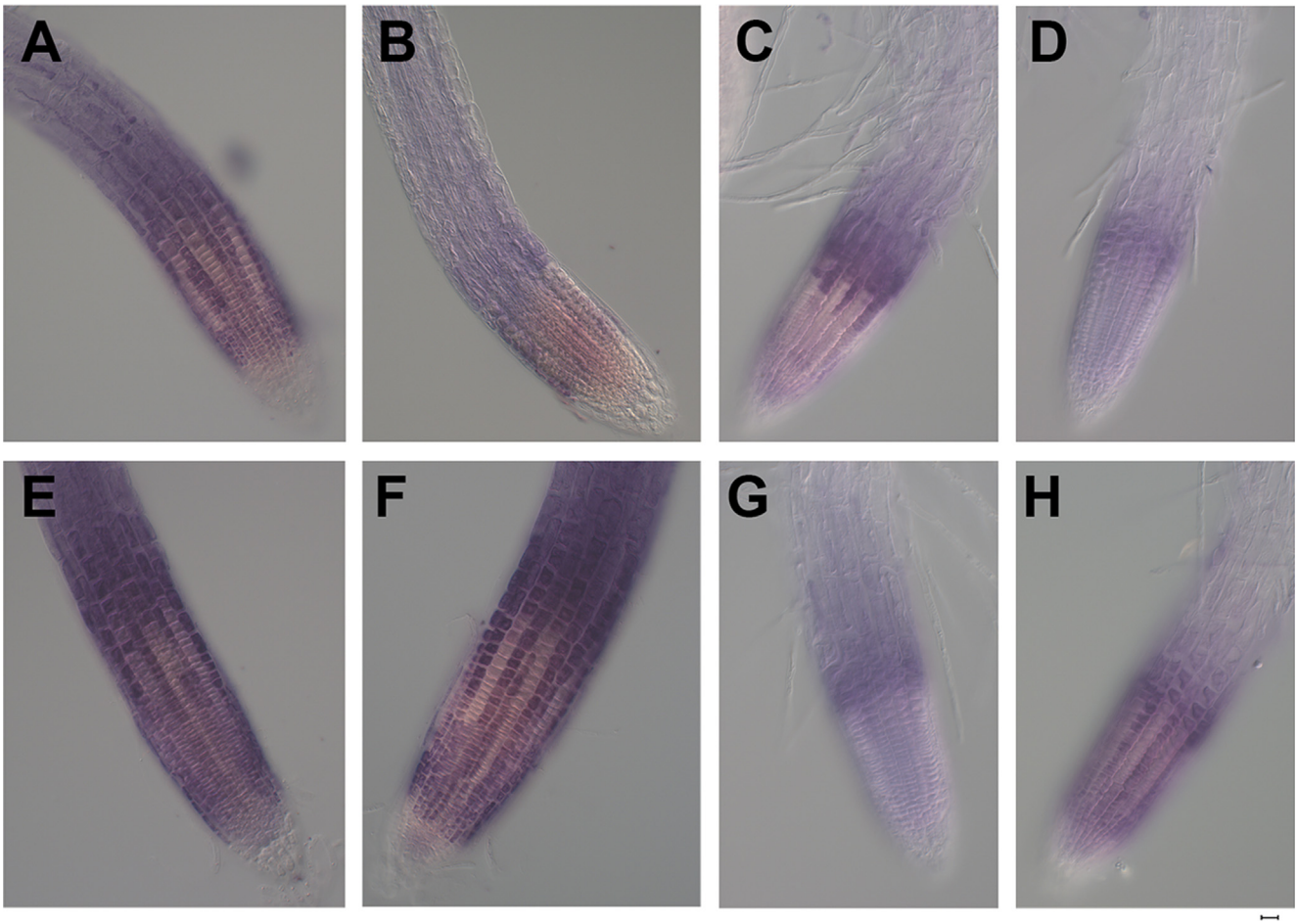

Fig. 5. Sucrose activates *CYCP*2;1 expression independent of STIP function. (A, B, E, and F) *CYCP*2;1 mRNA was detected using an anti-sense probe in 2-day-old *Col*-0 (A–E) and *stip*-1 (B–F) seedling roots, germinated on MS medium (A, and B) or MS medium supplement with 44 mM sucrose (E, and F). There is a visible increase in *CYCP*2;1 levels in samples grown on sugar-containing medium. (C, D, G, and H) *CYCP*2;1 mRNA was detected using an anti-sense probe in the roots of 1-day-old *Col*-0 (C) and *stip*-1 (D, G, and H) seedlings germinated on MS medium. Samples in (G and H) were treated with 44 mM sorbitol (G) or sucrose (H) for 2.5 h. All comparative samples were processed at the same time. Scale bar represents 20 μm.

dependent on the nature of its cyclin partner as previously suggested (Harashima and Schnittger, 2012).

Sucrose activates CYCP2;1 transcription independent of STIP

The evidence described above points to *CYCP2;*1 as a major component of the genetic pathway activated by STIP, which controls meristem growth activation after germination. A unique feature of the *stip* mutant seedling phenotype has been its full rescue by exogenously provided metabolic sugars (Wu et al., 2005). In addition, the STIP-independent increase in *CYCP2;*1 transcript levels after 72 h post-stratification (Fig. 1B) coincides with the full greening of the seedling, which signals the start of carbon fixation by photosynthesis. This raised the questions of the role *CYCP2;*1 plays in how sugar availability affects meristem cell cycle activities, and how it is related to STIP function. To answer these questions, we began by investigating whether sugar regulates *CYCP2;*1 expression in the root meristem region, where *CYCP2;*1 and *STIP* are expressed in overlapping domains throughout development.

Two days after germinating without exogenous sugar, *CYCP2;*1 mRNA can be detected in most of the cells in the root meristematic and transition zones in wildtype roots (Fig. 5A). In comparison, *CYCP*2;1 expression in wildtype seedlings germinated on sucrose-containing media is visibly higher, especially in the transition zone (Fig. 5E). A much more dramatic difference was observed in *stip* mutants of the same age. Without supplied sugar, very little *CYCP*2;1 transcript could be detected in *stip* roots (Fig. 5B), which already showed clear growth arrest. In contrast, *CYCP*2;1 expression in *stip* mutants germinated on sucrose media, which continued to develop, was indistinguishable from the wildtype samples both in amounts and the domain of expression (Fig. 5F, compare to E).

A potential concern with the above experiment is whether the observed *CYCP*2;1 activation by sugar is due to changes in cell type composition, especially in *stip* mutants. To address this issue, 1-day-old *stip*-1 seedlings that were germinated without sugar were treated with 44 mM sucrose or the osmotic control sorbitol for 2 ½ h and compared to ones without the treatment for *CYCP*2;1 expression. At this age, *CYCP*2;1 expression is concentrated near the transition zone in the wildtype roots (Fig. 5C). Without sugar, *CYCP*2;1 expression is already visibly reduced in *stip* roots (Fig. 5D). The brief sucrose treatment resulted in both an expansion of the *CYCP*2;1 domain and a clear increase of its expression levels (Fig. 5H). In comparison, the sorbitol treatment led to no change in *CYCP*2;1 expression in *stip* roots (Fig. 5G), suggesting that metabolic sugar is required for activating *CYCP*2;1 transcription. These results suggest that not only does sugar activate *CYCP*2;1 transcription independent of STIP in the root meristematic tissues, *CYCP*2;1 activation is also one of the early events in response to sugar signals. Furthermore, the activation of *CYCP*2;1 likely represents a key event in the sugar rescue of *stip* mutants.

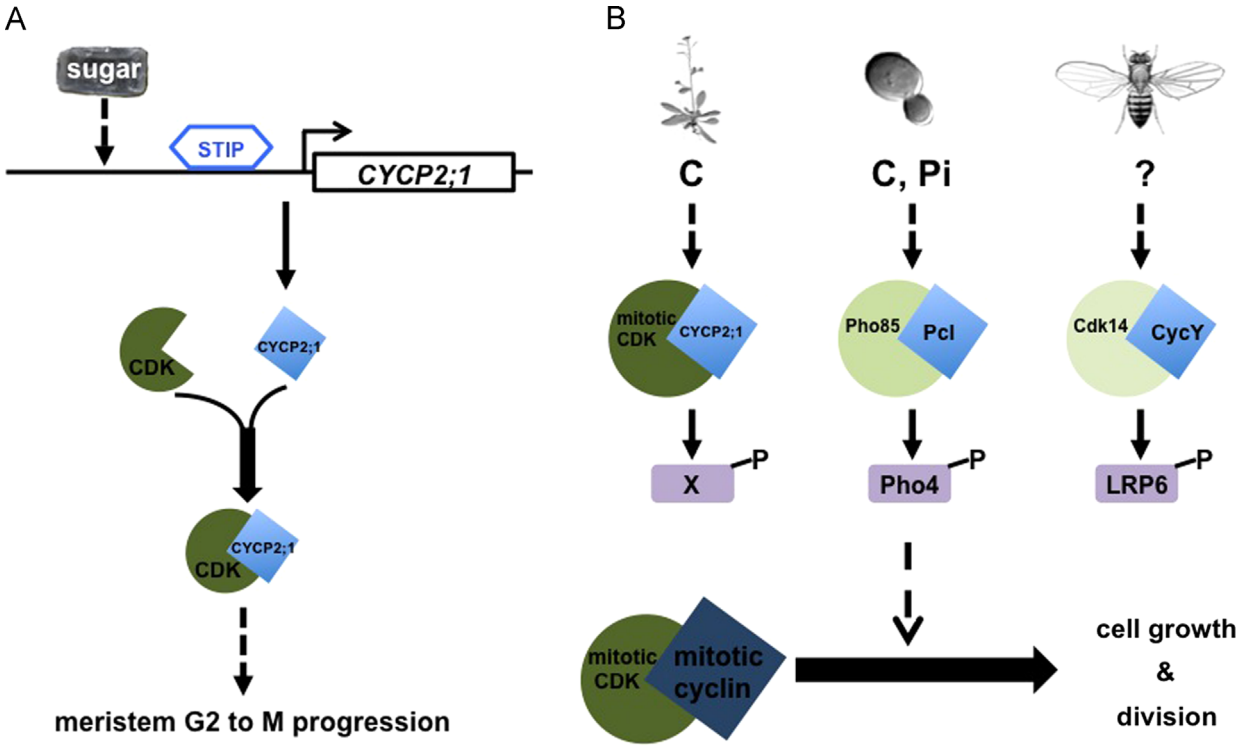

Fig. 6. Schematic representations of the mechanisms underlying the function of *CYCP*2;1 and its homologs in other organisms. (A) A summary of *CYCP*2;1 regulation and function in *Arabidopsis*. Both the homeobox transcription factor STIP and sugar signals are activators of *CYCP*2;1 transcription. However, as detailed in the discussion, the exact role of either factor is dependent upon both the tissue type (i.e. root v.s. shoot) and the developmental stage, specifically, before or after cotyledon greening. Once translated, the *CYCP*2;1 protein moves into the nucleus and forms protein complexes with CDKA;1, CDKB2;1, and CDKB2;2, which promote meristem cell cycle G2 to M transition at the time of germination. (B) A comparison of the role of Pcl-like cyclins in promoting cell growth and division based on nutritional information. In *S. cerevisiae* (center), the Pcl proteins dimerize with the non-essential CDK Pho85, which then phosphorylate the downstream targets including transcription factor Pho4. The activities of the Pho85-Pcl complexes are regulated by phosphate and carbohydrate availability. In *Arabidopsis* (left), *CYCP*2;1 is transcriptional activated by carbohydrate signals and it promotes cell cycle progression by physically interacts with three of the five mitotic CDKs. The *in vivo* kinase substrate of the *CYCP*2;1-CDK complexes remain to be determined. In *Drosophila* (right), the CycY-Cdk14 complex recruits Cdk14 to the plasma membrane, which results in the phosphorylation of LRP6 and the activation of the Wnt signaling pathway. It is currently unclear whether CycY expression or activity is regulated by nutrient availability.

In comparison, no significant change was observed in *CYCP*2;1 expression in the wildtype samples after both treatments (Fig. S3), which may be due to the presence of photosynthetic sugars in the wildtype cells or unknown mechanisms that limit the levels of *CYCP*2;1 expression.

Discussion

The activation of cell divisions in the primary meristems at the time of germination is an essential element of post-embryonic development in higher plants. Our previous work showed that both the homeobox transcription factor STIP and metabolic sugar signals play key roles in promoting this process at the G2 to M transition in *Arabidopsis* (Skylar et al., 2011; Wu et al., 2007, 2005). In this study, we present evidence that *CYCP*2;1 integrates both STIP and sugar signals in modulating meristem cell cycle activation (Fig. 6A).

CYCP2;1 is essential in post-embryonic meristem cell cycle G2 to M activation

The *Arabidopsis* P-family cyclins were initially identified through sequence homology and their ability to interact with CDKA;1 (Torres Acosta et al., 2004; Wang et al., 2004). However, the questions remain as to whether the CYCPs are involved in cell cycle regulation. Our finding that STIP binds to *CYCP*2;1 promoter and activates its early expression (Fig. 1) first hinted at a possible role for *CYCP*2;1 in meristem cell cycle activation. Additional evidence, including the high degree of similarity between the *stip* and *CYCP*2;1 mutants, nuclear DNA content analysis, and *CYCP*2;1's ability to partially complement the *stip* mutant phenotype, supports the conclusion that *CYCP*2;1 is a key activator of the G2 to M transition in the primary meristems at germination, and this function is likely to be carried out through its physical interaction with the G2/M-specific CDKs.

Compared to G1/S, the G2 to M transition in higher plants is much less understood, especially regarding the molecular function of the *B*-type CDKs. It has been proposed that CDKA and CDKB may play different roles in promoting cell cycle progression, with CDKB modulating CDKA activities (Francis, 2011). Consistent with this hypothesis, we found that *CYCP*2;1 and CYCD4;1 binding have different effects on the activities of the CDKs. CDKB2;1 was activated by both *CYCP*2;1 and CYCD4;1, which suggests that *CYCP*2;1-binding is equivalent to the binding of a mitotic cyclin in this case. In comparison, nearly no activation of CDKA;1 by *CYCP*2;1 was detected in our study, indicating that CDKA;1 responds differently to *CYCP*2;1 and a mitotic cyclin. These results raised additional questions about the mechanisms of *CYCP*2;1 function. For example, how does *CYCP*2;1-binding affect the binding of the mitotic cyclins to these CDKs? What is the function of *CYCP*2;1-binding if it does not activate a CDK? Additional studies are required to further understand the molecular function of *CYCP*2;1-CDK interaction. Furthermore, it is worth noting that the loss of CDKA;1 or the CDKB2s does not result in the failure of meristem activation at germination (Andersen et al., 2008; Nowack et al., 2012). Although we cannot exclude functional redundancy between the A and B type CDKs (Nowack et al., 2012) as the root cause of this phenotypic difference, it is likely

that *CYCP*2;1 carries out other functions in addition to binding CDK.

CYCP2;1 integrates genetic and nutritional information at transcriptional level

Based on their amino acid sequence homology to the yeast Pcl proteins, it has been postulated that the P-cyclins may regulate cell division based on nutrient status (Torres Acosta et al., 2004). Our findings show that *CYCP*2;1 fits in this functional category. More importantly, *CYCP*2;1 transcription is activated by both the sugar signals and STIP, making *CYCP*2;1 a point of integration of both intrinsic and nutritional cues. A closer examination reveals differences in how these two pathways are involved in activating *CYCP*2;1 expression, both spatially and temporally. A major dividing point in this process is approximately 72 h post-stratification, when the cotyledons of the newly germinated seedlings fully green. With *in situ* hybridization, *CYCP*2;1 mRNA was detected in the emerging seedlings starting no later than 48 h post-stratification, when germination is initiated. From this time until cotyledon greening, the *CYCP*2;1 expression domain overlaps with that of *STIP* (Fig. 1C–E), and *CYCP*2;1 expression is significantly reduced in *stip* mutants (Fig. 1B). Therefore, *STIP* plays the role of the main activator of *CYCP*2;1 during this period. Based on the results described in this study, we believe that this early *CYCP*2;1 expression is critical for primary meristem cell cycle activation, which has been shown to occur around the same time (Barroco et al., 2005). After cotyledon greening, *CYCP*2;1 expression is regulated differently in the shoot and the root. In the root, its expression domain continues to overlap with the *STIP* domain in the meristematic and transition zones, and is activated by both STIP and sugar signals (Fig. 5). In contrast, *STIP* most likely plays little to no role in activating *CYCP*2;1 expression in the shoot by this stage. Also at this time, a large increase in *CYCP*2;1 expression was observed in the shoot (Fig. 1B, data not shown). Although there is no direct evidence on the identity of *CYCP*2;1 activator in the shoot at this time, a good candidate is the photosynthetic sugar generated by the newly matured chloroplasts in the cotyledons. Further work is needed in understanding how the later phase of *CYCP*2;1 transcription in the shoot is regulated and in what way it is involved in maintaining tissue proliferation.

Pcl-like cyclins act as a permissive control of cell division

A living organism adjusts its growth and development in response to both intrinsic and environmental cues, and the state of the cell cycle is always a subject of these adjustments. The most understood unicellular experimental system in this respect is the budding yeast *S. cerevisiae*, in which the Pcl proteins interact with Pho85 to regulate cellular growth and division (Carroll and O'Shea, 2002; Kaffman et al., 1994; O'Neill et al., 1996). Although they are not part of the core cell cycle machinery, genetic analyses showed that five of the *Pcl* genes modulate cell cycle activities during the G1 phase based on nutrient availability and the loss of these genes results in growth retardation under certain conditions (Lee et al., 2000; Measday et al., 1997; Wang et al., 2001).

In higher plants, the meristems are the main tissues of cell division. A functional meristem must possess two basic features, tissue identity and cell cycle activities, both of which are reactivated at the time of germination. The patterning events define the cells within the meristems as undifferentiated and serve as the instructive control of any future cell divisions within meristematic tissues. Earlier reports have linked tissue identity genes to the activation of *CYCD*, which is required for the G1/S transition, in both the shoot and the root (Scofield et al., 2013; Sozzani et al., 2010). *CYCP*2;1, however, acts in a different branch of the regulatory network. Based on our expression analysis, *CYCP*2;1 does not interfere with the initial activation of many of the core cell cycle genes. Instead, it likely serves as a control mechanism for determining whether cell cycle should be allowed to proceed based on its upstream information, through modulating the activities of the G2/M mitotic CDKs. Consistent with this function, over-expression of *CYCP*2;1 caused no visible developmental change in wildtype plants. Interestingly, CDKB2;1 may play a similar role as *CYCP*2;1, since its transcription and protein stability may be controlled by a range of inputs (Adachi et al., 2011; Zhiponova et al., 2006). Therefore, one could envision the CDKB2;1-*CYCP*2;1 complex as one of the central hubs where genetic and environmental cues are incorporated to control the G2 to M transition in meristematic tissues.

A recent phylogenetic study of the Cyclin_N domain sequences from a large number of eukaryotes identified the highly conserved metazoan CycY as a member of the same clade as both Pcl and CYCP (Ma et al., 2013). It has been demonstrated that *Drosophila* CycY binds to and changes the subcellular localization of Cdk14, which results in the phosphorylation of one of the Wnt receptors and the activation of the Wnt signaling pathway in promoting tissue proliferation at the G2/M transition (Davidson et al., 2009; Liu and Finley, 2010). Although the exact molecular mechanisms underlying Pcl, *CYCP*2;1, and CycY function differ, these findings point to a common theme of the Pcl-family cyclins acting as permissive controls of cell proliferation, with the G2 to M transition being their target point in the multicellular organisms (Fig. 6B). Further studies of other member of this clade of genes are needed to test this hypothesis.

Acknowledgments

We thank Qiang Song and Andrew Smith for aligning the CHIP-seq reads; Olivier Brun for assisting with confocal imaging; Sarah Sabatinos for helping with flow cytometry analysis; Meng Chen and Fabien Pinaud for gifts of materials. This work was supported by grants from Academy of Sciences of the Czech Republic (M200201205 and RVO 61388971) to K.B. and a grant from NSF (MCB-1122213) to X.W. .

Appendix A. Supporting information

Supplementary data associated with this article can be found in the online version at http://dx.doi.org/10.1016/j.ydbio.2014.06.008.

References

Adachi, S., Minamisawa, K., Okushima, Y., Inagaki, S., Yoshiyama, K., Kondou, Y., Kaminuma, E., Kawashima, M., Toyoda, T., Matsui, M., et al., 2011. Programmed induction of endoreduplication by DNA double-strand breaks in *Arabidopsis*. Proc. Natl. Acad. of Sci. U.S.A. 108, 10004–10009.

Andersen, S.U., Buechel, S., Zhao, Z., Ljung, K., Novak, O., Busch, W., Schuster, C., Lohmann, J.U., 2008. Requirement of B2-type cyclin-dependent kinases for meristem integrity in *Arabidopsis thaliana*. Plant Cell 20, 88–100.

Barroco, R.M., Van Poucke, K., Bergervoet, J.H., De Veylder, L., Groot, S.P., Inze, D., Engler, G., 2005. The role of the cell cycle machinery in resumption of postembryonic development. Plant Physiol. 137, 127–140.

Bisova, K., Krylov, D.M., Umen, J.G., 2005. Genome-wide annotation and expression profiling of cell cycle regulatory genes in *Chlamydomonas reinhardtii*. Plant Physiol. 137, 475–491.

Boruc, J., Inze, D., Russinova, E., 2010. A high-throughput bimolecular fluorescence complementation protein-protein interaction screen identifies functional *Arabidopsis* CDKA/B-CYCD4/5 complexes. Plant Signal Behav. 5, 1276–1281.

Carroll, A.S., O'Shea, E.K., 2002. Pho85 and signaling environmental conditions. Trends Biochem. Sci. 27, 87–93.

Davidson, G., Shen, J., Huang, Y.L., Su, Y., Karaulanov, E., Bartscherer, K., Hassler, C., Stannek, P., Boutros, M., Niehrs, C., 2009. Cell cycle control of wnt receptor activation. Dev. Cell 17, 788–799.

De Veylder, L., Beeckman, T., Inze, D., 2007. The ins and outs of the plant cell cycle. Nat. Rev. Mol. Cell Biol. 8, 655–665.

Drummond-Barbosa, D., Spradling, A.C., 2001. Stem cells and their progeny respond to nutritional changes during *Drosophila* oogenesis. Dev. Biol. 231, 265–278.
Fankhauser, C., Chory, J., 1997. Light control of plant development. Annu. Rev. Cell Dev. Biol. 13, 203–229.
Francis, D., 2011. A commentary on the G(2)/M transition of the plant cell cycle. Ann. Bot. 107, 1065–1070.
Friml, J., Vieten, A., Sauer, M., Weijers, D., Schwarz, H., Hamann, T., Offringa, R., Jurgens, G., 2003. Efflux-dependent auxin gradients establish the apical-basal axis of *Arabidopsis*. Nature 426, 147–153.
Gaudin, V., Lunness, P.A., Fobert, P.R., Towers, M., Riou-Khamlichi, C., Murray, J.A., Coen, E., Doonan, J.H., 2000. The expression of D-cyclin genes defines distinct developmental zones in snapdragon apical meristems and is locally regulated by the *Cycloidea* gene. Plant Physiol. 122, 1137–1148.
Haecker, A., Gross-Hardt, R., Geiges, B., Sarkar, A., Breuninger, H., Herrmann, M., Laux, T., 2004. Expression dynamics of *WOX* genes mark cell fate decisions during early embryonic patterning in *Arabidopsis thaliana*. Development 131, 657–668.
Hanson, J., Smeekens, S., 2009. Sugar perception and signaling–an update. Curr. Opin. Plant Biol. 12, 562–567.
Harashima, H., Schnittger, A., 2012. Robust reconstitution of active cell-cycle control complexes from co-expressed proteins in bacteria. Plant Methods 8, 23.
Hemerly, A., Engler, J.d.A., Bergounioux, C., Van Montagu, M., Engler, G., Inze, D., Ferreira, P., 1995. Dominant negative mutants of the Cdc2 kinase uncouple cell division from iterative plant development. EMBO J. 14, 3925–3936.
Hu, C.D., Chinenov, Y., Kerppola, T.K., 2002. Visualization of interactions among bZIP and Rel family proteins in living cells using bimolecular fluorescence complementation. Mol. Cell 9, 789–798.
Inagaki, S., Umeda, M., 2011. Cell-cycle control and plant development. Int. Rev. Cell Mol. Biol. 291, 227–261.
Inzé, D., De Veylder, L., 2006. Cell cycle regulation in plant development. Ann. Rev. Genet. 40, 77–105.
Kaffman, A., Herskowitz, I., Tjian, R., O'Shea, E.K., 1994. Phosphorylation of the transcription factor PHO4 by a cyclin-CDK complex, PHO80-PHO85. Science 263, 1153–1156.
Komaki, S., Sugimoto, K., 2012. Control of the plant cell cycle by developmental and environmental cues. Plant Cel. Physiol. 53, 953–964.
Kono, A., Umeda-Hara, C., Lee, J., Ito, M., Uchimiya, H., Umeda, M., 2003. *Arabidopsis* D-type cyclin CYCD4;1 is a novel cyclin partner of B2-type cyclin-dependent kinase. Plant Physiol. 132, 1315–1321.
Lee, M., O'Regan, S., Moreau, J.L., Johnson, A.L., Johnston, L.H., Goding, C.R., 2000. Regulation of the Pcl7-Pho85 cyclin-cdk complex by Pho81. Mol. Microbiol. 38, 411–422.
Lees, E.M., Harlow, E., 1993. Sequences within the conserved cyclin box of human cyclin A are sufficient for binding to and activation of cdc2 kinase. Mol. Cell Biol. 13, 1194–1201.
Leibfried, A., To, J.P., Busch, W., Stehling, S., Kehle, A., Demar, M., Kieber, J.J., Lohmann, J.U, 2005. WUSCHEL controls meristem function by direct regulation of cytokinin-inducible response regulators. Nature 438, 1172–1175.
Lie, C., Kelsom, C., Wu, X., 2012. WOX2 and STIMPY-LIKE/WOX8 promote cotyledon boundary formation in *Arabidopsis*. Plant J. 72, 674–682.
Liu, D., Finley Jr., R.L., 2010. Cyclin Y is a novel conserved cyclin essential for development in *Drosophila*. Genet 184, 1025–1035.
Lorenz, S., Tintelnot, S., Reski, R., Decker, E.L., 2003. Cyclin D-knockout uncouples developmental progression from sugar availability. Plant Mol. Biol. 53, 227–236.
Ma, Z., Wu, Y., Jin, J., Yan, J., Kuang, S., Zhou, M., Zhang, Y., Guo, A.Y., 2013. Phylogenetic analysis reveals the evolution and diversification of cyclins in eukaryotes. Mol. Phylogenet. Evol. 66, 1002–1010.
Measday, V., Moore, L., Ogas, J., Tyers, M., Andrews, B., 1994. The PCL2 (ORFD)-PHO85 cyclin-dependent kinase complex: a cell cycle regulator in yeast. Science 266, 1391–1395.
Measday, V., Moore, L., Retnakaran, R., Lee, J., Donoviel, M., Neiman, A.M., Andrews, B., 1997. A family of cyclin-like proteins that interact with the Pho85 cyclin-dependent kinase. Mol. Cell Biol. 17, 1212–1223.
Medford, J.I., 1992. Vegetative apical meristems. Plant Cell 4, 1029–1039.
Menges, M., de Jager, S.M., Gruissem, W., Murray, J.A., 2005. Global analysis of the core cell cycle regulators of *Arabidopsis* identifies novel genes, reveals multiple and highly specific profiles of expression and provides a coherent model for plant cell cycle control. Plant J. 41, 546–566.
Moore, B., Zhou, L., Rolland, F., Hall, Q., Cheng, W.H., Liu, Y.X., Hwang, I., Jones, T., Sheen, J., 2003. Role of the *Arabidopsis* glucose sensor HXK1 in nutrient, light, and hormonal signaling. Science 300, 332–336.
Nowack, M.K., Harashima, H., Dissmeyer, N., Zhao, X., Bouyer, D., Weimer, A.K., De Winter, F., Yang, F., Schnittger, A., 2012. Genetic framework of cyclin-dependent kinase function in *Arabidopsis*. Dev. Cell 22, 1030–1040.
O'Neill, E.M., Kaffman, A., Jolly, E.R., O'Shea, E.K., 1996. Regulation of PHO4 nuclear localization by the PHO80-PHO85 cyclin-CDK complex. Science 271, 209–212.
Paul, M.J., Primavesi, L.F., Jhurreea, D., Zhang, Y., 2008. Trehalose metabolism and signaling. Annu. Rev. Plant Biol. 59, 417–441.
Porceddu, A., Stals, H., Reichheld, J.P., Segers, G., De Veylder, L., Barroco, R.P., Casteels, P., Van Montagu, M., Inze, D., Mironov, V., 2001. A plant-specific cyclin-dependent kinase is involved in the control of G2/M progression in plants. J. Biol. Chem. 276, 36354–36360.
Puthiyaveetil, S., Allen, J.F., 2008. Transients in chloroplast gene transcription. Biochem. Biophys. Res. Commun. 368, 871–874.
Rieu, I., Laux, T., 2009. Signaling pathways maintaining stem cells at the plant shoot apex. Semin. Cell Dev. Biol. 20, 1083–1088.
Riou-Khamlichi, C., Menges, M., Healy, J.M., Murray, J.A., 2000. Sugar control of the plant cell cycle: differential regulation of *Arabidopsis* D-type cyclin gene expression. Mol. Cell Biol. 20, 4513–4521.
Scofield, S., Dewitte, W., Nieuwland, J., Murray, J.A., 2013. The *Arabidopsis* homeobox gene *SHOOT MERISTEMLESS* has cellular and meristem-organisational roles with differential requirements for cytokinin and CYCD3 activity. Plant J. 75, 53–66.
Sessions, A, Weigel, D., Yanofsky, M.F., 1999. The *Arabidopsis thaliana MERISTEM LAYER* 1 promoter specifies epidermal expression in meristems and young primordia. Plant J. 20, 259–263.
Shim, Y.H., Chun, J.H., Lee, E.Y., Paik, Y.K., 2002. Role of cholesterol in germ-line development of *Caenorhabditis elegans*. Mol. Reprod. Dev. 61, 358–366.
Skylar, A., Hong, F., Chory, J., Weigel, D., Wu, X., 2010. STIMPY mediates cytokinin signaling during shoot meristem establishment in *Arabidopsis* seedlings. Development 137, 541–549.
Skylar, A., Sung, F., Hong, F., Chory, J., Wu, X., 2011. Metabolic sugar signal promotes *Arabidopsis* meristematic proliferation via G2. Dev. Biol. 351, 82–89.
Smith, A.D., Xuan, Z., Zhang, M.Q., 2008. Using quality scores and longer reads improves accuracy of Solexa read mapping. BMC Bioinform. 9, 128.
Sozzani, R., Cui, H., Moreno-Risueno, M.A., Busch, W., Van Norman, J.M., Vernoux, T., Brady, S.M., Dewitte, W., Murray, J.A., Benfey, P.N., 2010. Spatiotemporal regulation of cell-cycle genes by *SHORTROOT* links patterning and growth. Nature 466, 128–132.
Steeves, T.A., Sussex, I.M., 1989. Patterns in Plant Development, 2nd edn, Cambridge University Press, Cambridge, UK.
Torres Acosta, J.A., de Almeida Engler, J., Raes, J., Magyar, Z., De Groodt, R., Inze, D., De Veylder, L., 2004. Molecular characterization of *Arabidopsis* PHO80-like proteins, a novel class of CDKA;1-interacting cyclins. Cell Mol. Life Sci. 61, 1485–1497.
Van't Hof, J., 1966. Experimental control of Dna synthesizing and dividing cells in excised root tips of pisum. Am. J. Bot. 53, 970–976.
Veit, B., 2004. Determination of cell fate in apical meristems. Curr. Opin. Plant. Biol. 7, 57–64.
Voinnet, O., Rivas, S., Mestre, P., Baulcombe, D., 2003. An enhanced transient expression system in plants based on suppression of gene silencing by the p19 protein of tomato bushy stunt virus. Plant J. 33, 949–956.
Wang, G., Kong, H., Sun, Y., Zhang, X., Zhang, W., Altman, N., DePamphilis, C.W., Ma, H., 2004. Genome-wide analysis of the cyclin family in *Arabidopsis* and comparative phylogenetic analysis of plant cyclin-like proteins. Plant Physiol. 135, 1084–1099.
Wang, Z., Wilson, W.A., Fujino, M.A., Roach, P.J., 2001. The yeast cyclins Pc16p and Pc17p are involved in the control of glycogen storage by the cyclin-dependent protein kinase Pho85p. FEBS Lett. 506, 277–280.
Wu, X., Chory, J., Weigel, D., 2007. Combinations of WOX activities regulate tissue proliferation during *Arabidopsis* embryonic development. Dev. Biol. 309, 306–316.
Wu, X., Dabi, T., Weigel, D., 2005. Requirement of homeobox gene *STIMPY/WOX*9 for *Arabidopsis* meristem growth and maintenance. Curr. Biol. 15, 436–440.
Wu, X., Dinneny, J.R., Crawford, K.M., Rhee, Y., Citovsky, V., Zambryski, P.C., Weigel, D., 2003. Modes of intercellular transcription factor movement in the *Arabidopsis* apex. Development 130, 3735–3745.
Yoo, S.Y., Bomblies, K., Yoo, S.K., Yang, J.W., Choi, M.S., Lee, J.S., Weigel, D., Ahn, J.H., 2005. The 35S promoter used in a selectable marker gene of a plant transformation vector affects the expression of the transgene. Planta 221, 523–530.
Zhiponova, M.K., Pettko-Szandtner, A., Stelkovics, E., Neer, Z., Bottka, S., Krenacs, T., Dudits, D., Feher, A., Szilak, L., 2006. Mitosis-specific promoter of the alfalfa cyclin-dependent kinase gene (Medsa;CDKB2;1) is activated by wounding and ethylene in a non-cell division-dependent manner. Plant Physiol. 140, 693–703.